

*Physics*

*Physics Research Publications*

---

*Purdue University*

*Year* 2007

---

Natural focusing of x rays from  
ferroelectric lithium niobate wafers

S. Durbin

T. Jach

S. Kim

V. Gopalan

This paper is posted at Purdue e-Pubs.

[http://docs.lib.purdue.edu/physics\\_articles/627](http://docs.lib.purdue.edu/physics_articles/627)

# Natural focusing of x rays from ferroelectric lithium niobate wafers

Stephen Durbin<sup>a)</sup>

*Department of Physics, Purdue University, West Lafayette, Indiana 47907-2036, USA*

Terrence Jach

*Chemical Science and Technology Laboratory, National Institute of Standards and Technology, Gaithersburg, Maryland 20899-8371, USA*

Sungwon Kim<sup>b)</sup> and Venkatraman Gopalan

*Materials Research Institute and Department of Materials Science and Engineering, Pennsylvania State University, University Park, Pennsylvania 16802, USA*

(Received 28 August 2007; accepted 14 September 2007; published online 5 October 2007)

The interaction of waves with inhomogeneous media leads to the natural focusing of light, the channelling of waves into stable caustics. We have extended natural focusing to x rays, observing caustics in topographs of ferroelectric lithium niobate. Voltage across domains of reversed polarity induces perturbations to the local crystal planes, producing dramatic variations in the images. Ray tracing shows a “catastrophic” discontinuity, causing bright focal lines. Analysis reveals details of boundary strains and local ferroelectric properties. Controlled focusing could be extended to designed domain patterns to probe microstructural properties, and also to a type of voltage-controlled ferroelectric optics for x rays. © 2007 American Institute of Physics.

[DOI: [10.1063/1.2794404](https://doi.org/10.1063/1.2794404)]

Light interacting with materials leads to caustics, a natural focusing into stable lines with a variety of possible topological features.<sup>1,2</sup> This is a universal phenomenon observed in the reflection of sunlight from surface ripples in water, from water droplets on a sheet of glass, and many other situations that arise without highly engineered optical elements. The study of natural focusing goes back at least as far as da Vinci’s sketches of the familiar cusp of light reflected from the interior of a drinking cup.<sup>2</sup> Caustics describe the multiple imaging of galaxies associated with gravitational lensing and are now included in discussions of cosmological dark matter.<sup>3–7</sup> A mathematical foundation is provided by catastrophe theory.<sup>8,9</sup> (The notion of “catastrophe” can be seen in a geometrical ray model, where a point on an image is abruptly illuminated by two or more intersecting rays instead of just one: the intensity discontinuity is said to be catastrophic.) Recent studies have established many phenomena predicted by theory.<sup>10–14</sup>

In this work, we report the observation of caustics at x-ray wavelengths using diffraction from ferroelectric wafers. We employ x-ray topography to investigate lithium niobate, a widely used ferroelectric material. Ideally, an x-ray topograph uses a monochromatic plane wave beam to diffract off a set of crystal planes. If the specimen is an ideal crystal and the beam is at the Bragg angle, the reflected beam will be recorded as an image of uniform illumination. In real specimens, intensity modulations can arise from various imperfections, allowing routine imaging of dislocations and other microstructures.<sup>15</sup>

Lithium niobate has a noncentrosymmetric unit cell (3m point group symmetry) with a permanent electric polarization,<sup>16,17</sup> so an applied electric field causes piezoelec-

tric expansion or contraction of the crystal. Wafers can be “unpoled” with no intentional alignment of the polarization, “poled” or polarized so that the wafer is a single domain of parallel polarization, or “reverse poled” where it is first uniformly poled and then local domains have the polarization reversed by a large electric field. When a uniform electric field is applied to a reverse-poled wafer, the matrix may expand, while the reverse-poled domains contract (or *vice versa*, depending on field direction). The induced curvature is discernable with topography.<sup>18–21</sup>

We used congruent lithium niobate, a standard material with Li vacancies and Nb antisite occupation in concentrations given by  $(\text{Li}_{0.95}\text{Nb}_{0.01})\text{NbO}_3$ .<sup>17</sup> X-ray topographs of a 300  $\mu\text{m}$  thick wafer are shown in Fig. 1. The top image is a standard Bragg-geometry [00.12] topograph with 8.5 keV x rays, obtained with an x-ray camera with 6  $\mu\text{m}$  resolution, located 0.47 m from the specimen. This wafer is reverse poled, with the right half of the image covered by one large hexagonal domain, and a number of small domains distributed throughout the matrix in the left side.

Dramatic and apparently nonlinear responses are seen as voltage is applied across the wafer (after electrical contacts were made to thin films of sputtered carbon on opposite faces), first exhibited as a slight bulging of the matrix (1500 V), then a convergence into bright lines separated by dark regions (3000 and 3500 V), and finally, just a few sharp features above a mostly dark background (4000 V). The behavior is reversible: cycling back down to 0 V and back yielded nearly identical images. These images cannot be attributed to any real motion of domain walls in response to the applied electric field, as it was previously determined that domains walls remained fixed with respect to immobile dislocations,<sup>18,19,22</sup> and domain growth from large coercive fields is inconsistent with the observed reversibility. (The coercive field for domain wall motion in congruent lithium niobate at room temperature is  $\sim 21$  kV/mm,<sup>23</sup> higher than the maximum of 13.3 kV/mm applied here.)

<sup>a)</sup>Present address: Intel Corporation, Advanced Design Group, Hillsboro, OR 97124, USA.

<sup>b)</sup>Author to whom correspondence should be addressed. Electronic mail: [durbin@physics.purdue.edu](mailto:durbin@physics.purdue.edu)

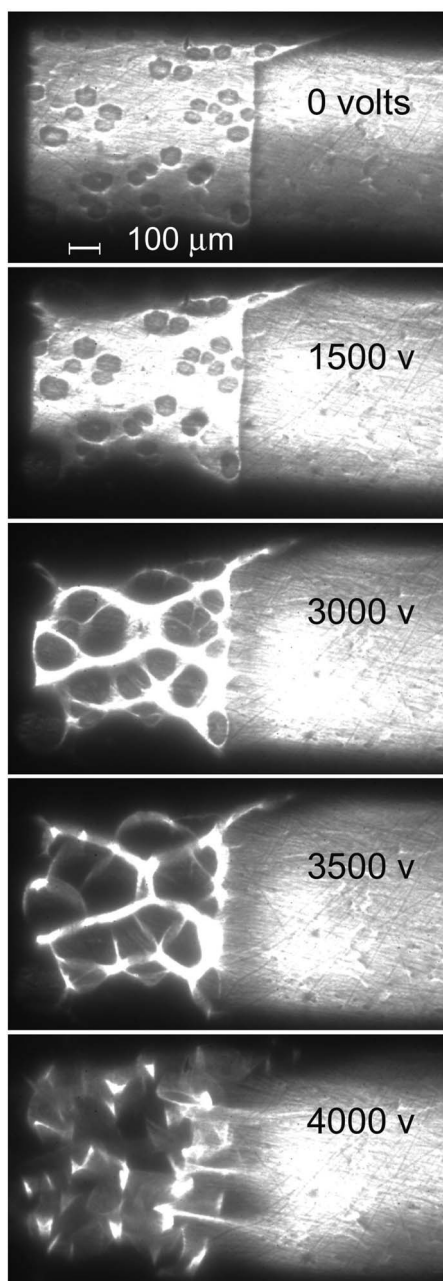


FIG. 1. X-ray catastrophe focusing from reversed domains in lithium niobate. Top panel is an 8.5 keV x-ray topograph of the [00.12] reflection from a reverse-poled 300  $\mu\text{m}$  thick lithium niobate *c*-axis wafer oriented on a six-circle diffractometer, recorded with an x-ray camera having a 6  $\mu\text{m}$  pixel size and using a 0.05 s exposure time. One large hexagonal domain covers the right half, with numerous small domains on the left. (Scale bar denotes 100  $\mu\text{m}$ .) Carbon films were deposited on opposite wafer faces, providing electrically conducting surfaces transparent to the x rays. Succeeding panels were obtained with static applied voltages as labeled, showing a gradual focusing into caustics. Images acquired with an undulator and Si(111) monochromator at Sector 1 of the Advanced Photon Source (Argonne).

A monochromatic plane wave is specularly reflected with respect to the crystal planes responsible for diffraction. If a given domain is tilted slightly with respect to the average wafer orientation, any x rays reflected from that domain will travel in a slightly different direction. The reflectivity quickly drops to zero away from the Bragg angle, so this change of direction can only be a factor for tilt angles smaller than the local reflectivity width, which is 16.3  $\mu\text{rad}$  for the [00.12] reflection of perfect  $\text{LiNbO}_3$ . Measured rocking curves for this and similar wafers ranged from 25 to 130  $\mu\text{rad}$ .

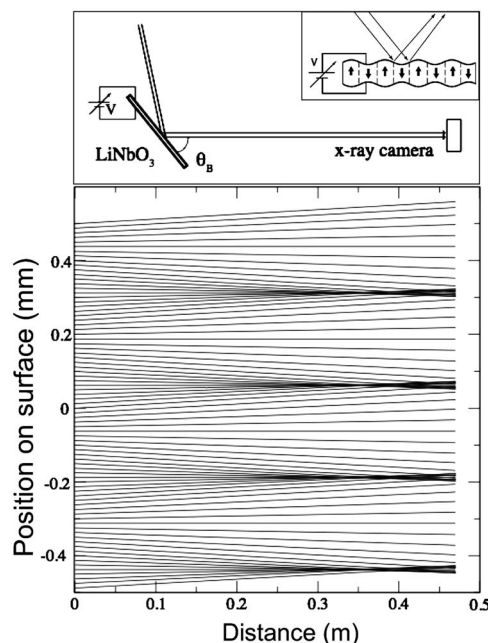


FIG. 2. Ray-tracing model of x-ray caustic formation. Main panel traces a set of x rays specularly reflected from a sinusoidally modulated surface, with the *y* axis greatly expanded (millimeter units) compared to the *x* axis (meters). Top panel shows the simple diffraction geometry, with undulator radiation well approximated as ideal parallel rays diffracting from a lithium niobate wafer with a controllable applied voltage across its thickness; inset indicates the periodic ferroelectric domain reversal pattern.

Adjacent domains of opposite polarity will have identical lattice constants and continuous lattice planes across the ferroelectric domain boundary in the absence of an applied electric field. The contraction and expansion on opposing sides of the domain boundary due to an electric field cause bending of the crystal planes. We have modeled the effect of a sinusoidal modulation of lattice planes (Fig. 2). Plane waves at the average Bragg angle strike a crystal with a sinusoidal lattice modulation,  $y(x) = A \sin(2\pi x/\lambda)$ . Choosing  $\lambda = 400 \mu\text{m}$  and  $A = 4.0 \text{ nm}$  yields a maximum lattice plane slope of 62  $\mu\text{rad}$ ; slopes much larger than this would be outside the observed rocking curve widths. Imposing specular reflectivity, we plot the reflected ray from the sample surface to an image plane 0.5 m away. Rays are deflected to form caustics, with a singularity (catastrophe) at  $x \sim 0.35 \text{ m}$  where rays intersect. This simple model is thus sufficient to simulate the type of caustics observed in Fig. 1, where the camera distance was 0.47 m.

The simulation indicates that the features shown at high voltages in Fig. 1 are associated with surface height displacements on the order of  $A = 4 \text{ nm}$ . (For a more mathematical treatment of a related system with visible light, see Ref. 24.) The bulk piezoelectric constant for lithium niobate is  $d_{333} = 0.6 \times 10^{-11} \text{ C/N}$ , so at 3500 V a uniform wafer would change thickness by 21 nm. If a domain is small enough that long-range strains caused by the domain boundaries affect the whole domain, however, the amplitude  $A$  will be reduced. Earlier image analysis employing kinematic diffraction and finite element analysis also showed that the piezoelectric response of reverse-poled domains was smaller than predicted, even taking into account expected shear coefficients at the boundaries.<sup>19</sup>

Note that increasing the voltage is equivalent to moving the camera to greater distances  $R$  in Fig. 2. The top panel in Fig. 1 corresponds to the ray pattern close to  $R = 0$ , the panel



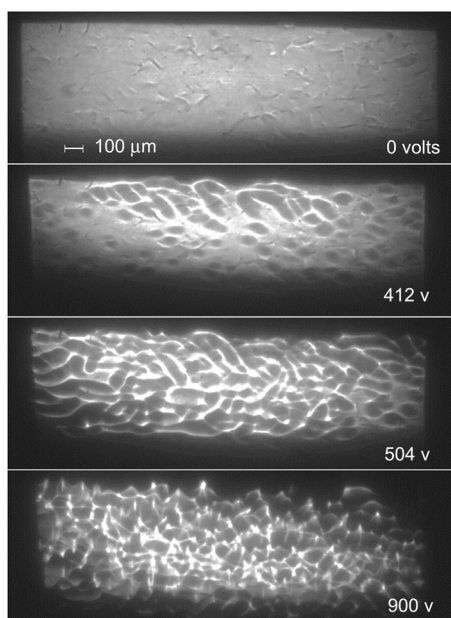


FIG. 3. Caustic formation from induced domains in unpoled lithium niobate. Top panel is an x-ray topograph of a 100  $\mu\text{m}$  thick lithium niobate wafer that had not been initially polarized. (Scale bar denotes 100  $\mu\text{m}$ .) Subsequent panels with 412, 504, and 900 V reveal reversible caustic formation associated with induced domains of opposite polarities.

at 3500 V corresponds to putting the camera near the ray crossing point at 0.35 m, and the image at 4000 V shows caustic behavior found at  $R=0.47$  m, where folds are evident. Thus Fig. 1 could also have been obtained by keeping the voltage fixed at a high value (e.g., 4000 V) and moving the camera to different values of  $R$ .

Topographs were also obtained from an unpoled 100  $\mu\text{m}$  wafer of  $c$ -axis congruent lithium niobate (with the same beamline configuration as before). The top panel in Fig. 3 shows a standard x-ray topograph with no applied voltage, exhibiting minor surface imperfections but no identifiable domains on the scale of 6  $\mu\text{m}$  resolution of these images. Voltage-induced focusing behavior quickly appears, as shown by topographs of 412, 504, and 900 V. The maximum applied field (of  $\sim 9$  kV/mm) is still significantly below the coercive field ( $\sim 21$  kV/mm) for this material. These striking images were also reversible for this range of voltages. Clearly the same type of modulation caused by the reverse poled domains in Fig. 1 is seen here, with a similar length scale and electric field dependence, but there are no reversed domains evident in the topograph. This raises the question: how does the specimen organize itself into competing domains upon the application of an electric field? One possibility is that there exist polarized microdomains stabilized by defects such as dislocations and low angle grain boundaries. Such microdomains typically act as nucleation sites for domain reversal in poled wafers. Microdomains smaller than the 6  $\mu\text{m}$  pixel size cannot be seen, but under an external electric field, the associated piezoelectric strain may contribute to the observed polarization effects.<sup>21,25</sup>

This configuration of ferroelectric crystalline wafer in an undulator x-ray beam provides a simple yet powerful tool for generating catastrophe focusing controllable by voltage alone. Image analysis provides quantitative details of local surface curvature and displacements that can be used to assess the long-range strains associated with domain boundaries and to uncover new phenomena such as the organiza-

tion of unpoled material into domains. It would be straightforward to extend these investigations to periodically poled specimens, fabricated with parallel reversed stripes.<sup>26,27</sup> Measuring the curvature induced by a given field as a function of the stripe width would directly yield the range of strains induced by the domain boundaries. Although an essential feature of caustics is their stability against generic perturbations of the material (unlike the focusing of a lens, for example), there is something to gain by engineering in some material features. Investigating domain boundary properties with a periodically poled wafer might be a first step toward engineering a pattern of domains with a specific geometry that could be used to focus an x-ray beam into a specific shape or profile. The ability to tilt the planes of small domains within a single wafer may be a useful degree of freedom for the development of controllable x-ray optics.

Research was supported by DOE (S. D. and T. J.) and NSF Grant Nos. DMR0602986, 0512165, 0512165, and 0213623 (S. K. and V. G.). Use of the Advanced Photon Source was supported by the U.S. Department of Energy, Office of Science, Office of Basic Energy Sciences, under Contract No. DE-AC02-06CH11357.

<sup>1</sup>M. V. Berry and C. Upstill, in *Progress in Optics*, edited by E. Wolf (North-Holland, Amsterdam, 1980), Vol. 18, p. 257.

<sup>2</sup>J. F. Nye, *Natural Focusing and Fine Structure of Light: Caustics and Wave Dislocations* (Taylor & Francis, London, 1999).

<sup>3</sup>T. H. Yano, H. Koyama, T. Buchert, and N. Gouda, *Astrophys. J., Suppl. Ser.* **151**, 185 (2004).

<sup>4</sup>S. J. Chung, C. Han, B. G. Park, D. Kim, and S. Kang, *Astrophys. J.* **630**, 535 (2005).

<sup>5</sup>A. Diaferio, M. J. Geller, and K. J. Rines, *Astrophys. J.* **628**, L97 (2005).

<sup>6</sup>R. Gavazzi, R. Mohayaee, and B. Fort, *Astron. Astrophys.* **445**, 43 (2006).

<sup>7</sup>A. Natarajan and P. Sikivie, *Phys. Rev. D* **73**, 023510 (2006).

<sup>8</sup>R. Thom, *Structural Theory and Morphogenesis: An Outline of a General Theory of Models* (Benjamin Cummings, Reading, MA, 1975).

<sup>9</sup>V. I. Arnold, *Singularities of Caustics and Wavefronts* (Kluwer, Dordrecht, 1990).

<sup>10</sup>M. V. Berry and F. J. Wright, *Philos. Trans. R. Soc. London, Ser. A* **291**, 453 (1979).

<sup>11</sup>M. V. Berry and E. Bodenschatz, *J. Mod. Opt.* **46**, 349 (1999).

<sup>12</sup>M. V. Berry, *New J. Phys.* **4**, 74 (2002).

<sup>13</sup>J. F. Nye, *J. Opt. A, Pure Appl. Opt.* **5**, 503 (2003).

<sup>14</sup>J. F. Nye, *Proc. R. Soc. London, Ser. A* **463**, 343 (2007).

<sup>15</sup>K. D. Bowen and B. K. Tanner, *High Resolution X-ray Diffractometry and Topography* (Taylor & Francis, Bristol, PA, 1998).

<sup>16</sup>H. D. Megaw, *Acta Crystallogr., Sect. A: Cryst. Phys., Diff., Theor. Gen. Crystallogr.* **A24**, 583 (1968).

<sup>17</sup>P. Lerner, C. Legras, and J. P. Dumas, *J. Cryst. Growth* **3-4**, 231 (1968).

<sup>18</sup>T. Jach, S. Kim, S. Durbin, V. Gopalan, and D. Bright, in *Fundamental Physics of Ferroelectrics*, edited by R. E. Cohen (AIP, Melville, NY, 2002), Vol. 626, p. 260.

<sup>19</sup>T. Jach, S. Kim, V. Gopalan, S. Durbin, and D. Bright, *Phys. Rev. B* **69**, 064113 (2004).

<sup>20</sup>P. Rejmankova, J. Baruchel, P. Moretti *et al.*, *J. Appl. Crystallogr.* **31**, 106 (1998).

<sup>21</sup>P. Pernot-Rejmankova, W. Laprus, and J. Baruchel, *Eur. Phys. J.: Appl. Phys.* **8**, 225 (1999).

<sup>22</sup>T. Jach, S. Durbin, S. Kim, and V. Gopalan, in *Electroceramic Materials and Applications*, Ceramic Transactions, edited by R. W. Schwartz, Ceramic Transactions (American Ceramics Society, Westerville, OH, 2006), Vol. 196, p. 119.

<sup>23</sup>S. Kim, V. Gopalan, and A. Gruverman, *Appl. Phys. Lett.* **80**, 2740 (2002).

<sup>24</sup>M. V. Berry, *Eur. J. Biochem.* **27**, 109 (2006).

<sup>25</sup>M. Yamada, N. Nada, M. Saitoh, and K. Watanabe, *Appl. Phys. Lett.* **62**, 435 (1993).

<sup>26</sup>M. Drakopoulos, Z. W. Hu, S. Kuznetsov, A. Snigirev, I. Snigirev, and P. A. Thomas, *J. Phys. D* **32**, A160 (1999).

<sup>27</sup>R. G. Batchko, V. Y. Shur, M. M. Fejer, and R. L. Byer, *Appl. Phys. Lett.* **75**, 1673 (1999).